IEEE Photonics Journal
An IEEE Photonics Society Publication

Open Access

# Achieving Uniform Carrier Distribution in MBE-Grown Compositionally Graded InGaN Multiple-Quantum-Well LEDs

Volume 7, Number 3, June 2015

**Pawan Mishra, Student Member, IEEE**
**Bilal Janjua, Student Member, IEEE**
**Tien Khee Ng, Member, IEEE**
**Chao Shen, Student Member, IEEE**
**Abdelmajid Salhi, Member, IEEE**
**Ahmed Y. Alyamani**
**Munir M. El-Desouki, Member, IEEE**
**Boon S. Ooi, Senior Member, IEEE**

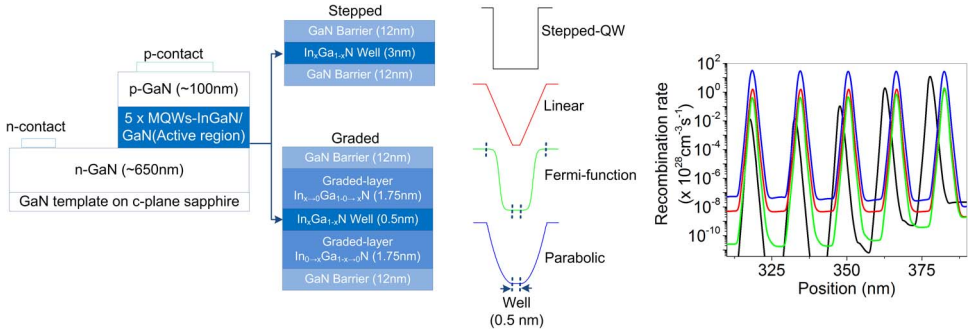


DOI: 10.1109/JPHOT.2015.2430017
1943-0655 

IEEE photonics SOCIETY

IEEE

# Achieving Uniform Carrier Distribution in MBE-Grown Compositionally Graded InGaN Multiple-Quantum-Well LEDs

**Pawan Mishra,[1] *Student Member, IEEE*, Bilal Janjua,[1] *Student Member, IEEE*, Tien Khee Ng,[1] *Member, IEEE*, Chao Shen,[1] *Student Member, IEEE*, Abdelmajid Salhi,[2] *Member, IEEE*, Ahmed Y. Alyamani,[2] Munir M. El-Desouki,[2] *Member, IEEE*, and Boon S. Ooi,[1] *Senior Member, IEEE***

[1]Photonics Laboratory, Computer, Electrical and Mathematical Sciences and Engineering Division, King Abdullah University of Science and Technology (KAUST), Thuwal 23955-6900, Saudi Arabia
[2]National Center for Nanotechnology, King Abdulaziz City for Science and Technology (KACST), Riyadh 11442-6086, Saudi Arabia

*DOI: 10.1109/JPHOT.2015.2430017*


Manuscript received April 12, 2015; revised April 30, 2015; accepted May 1, 2015. Date of publication May 6, 2015; date of current version May 18, 2015. This work was supported in part by King Abdullah University of Science and Technology (KAUST) baseline funding and in part by the King Abdulaziz City for Science and Technology (KACST) Technology Innovation Center for Solid State Lighting at KAUST. Corresponding author: B. S. Ooi (e-mail: boon.ooi@kaust.edu.sa).

**Abstract:** We investigated the design and growth of compositionally graded InGaN multiple-quantum-well (MQW)-based light-emitting diodes (LEDs) without an electron-blocking layer. Numerical investigation showed uniform carrier distribution in the active region and higher radiative recombination rate for the optimized graded-MQW design, i.e., $In_{0\rightarrow x}Ga_{1\rightarrow(1-x)}N/In_xGa_{(1-x)}N/In_{x\rightarrow 0}Ga_{(1-x)\rightarrow 1}N$, as compared with the conventional stepped-MQW-LED. The composition-grading schemes, such as linear, parabolic, and Fermi-function profiles, were numerically investigated for comparison. The stepped- and graded-MQW-LEDs were then grown using plasma-assisted molecular beam epitaxy through surface-stoichiometry optimization based on reflection high-energy electron diffraction *in situ* observations. Stepped- and graded-MQW-LED showed efficiency roll over at 160 and 275 A/cm$^2$, respectively. The extended threshold current density roll-over (droop) in graded-MQW-LED is due to the improvement in carrier uniformity and radiative recombination rate, which is consistent with the numerical simulation.

**Index Terms:** Compositional grading, light-emitting diodes (LEDs), polarization field, semiconductor quantum well, solid-state lighting, wavefunction overlap.

## 1. Introduction

Despite InGaN-based light-emitting diodes (LEDs) being the key driver for solid-state lighting technology, the device performance at high injection current density is limited by efficiency droop. A number of possible mechanisms had been suggested to account for the droop, summarized as follows: Auger recombination [1], carrier delocalization [2], and current injection efficiency quenching [3]. The severe band bending in c-plane InGaN/GaN multiple quantum well (MQW) arising from the built-in spontaneous and piezoelectric polarization fields [4]–[6] was also accounted for the major root cause of the issue. As the severe band banding leads to the reduced oscillator strength,

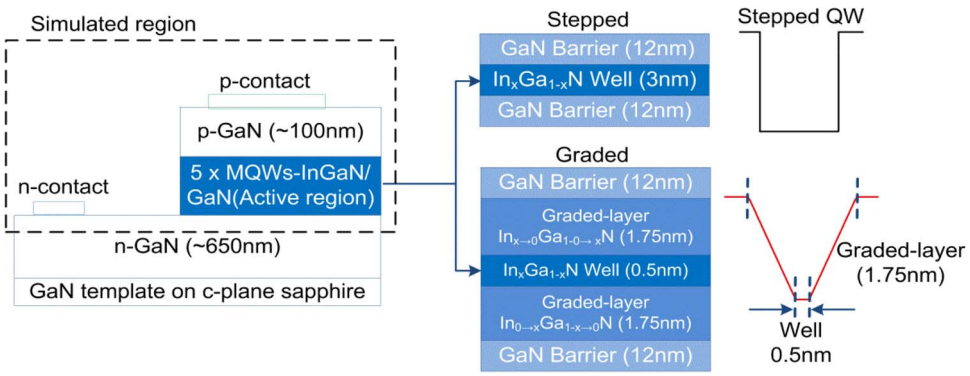


Fig. 1. Schematic diagram of the InGaN LED structures with stepped-MQW and the compositionally graded-MQW.

which is inversely proportional to the spatial electron-hole separation, non-uniform distribution of carriers in MQW, and electron leakage, especially at the QW closest to p-GaN [7]–[9].

In typical LED structures, the electron blocking layer (EBL) has been incorporated between the active region and p-GaN to increase overall carrier concentration by reflecting electrons back into the active region. The downside of the EBL scheme is the reduction of the hole injection efficiency, due to severe band bending and valance band (VB) offset at AlGaN/GaN interface which can promote electron leakage [10]–[12]. Solutions suggested to partly mitigate the side-effects of EBL are: graded-EBL [13], lattice-matched InAlN-EBL [14], [15], superlattice-EBL [16], [17] and, graded-superlattice-EBL [8], [18]. EBL-less designs based on insertion of undoped-GaN-layer in between active-region and p-GaN layer [19], GaN–AlGaN–GaN as last barrier [20], AlGaN-step-like-barriers [21], thin-AlGaN-barriers [22], specially-designed p-InGaN barrier [23], and two-step Mg-doped p-GaN [24] were also proposed to improve carrier confinement. Although the carrier concentration improves in these theoretical and experimental studies, the issues of non-uniform carrier distribution remain, which may again lead to efficiency droop of MQW. Thus, active region design that promotes uniform carriers distribution for reducing electron leakage, and improving hole injection become important. One of the possible ways to increase the output power and alleviate efficiency droop, is to improve the wavefunction overlap in the InGaN QWs by using QWs with non-conventional shapes [25]–[31], semi-polar [32], [33] or non-polar [34], [35] QWs as active material in LED structures. InGaN/GaN graded MQW LED with EBL based on linear grading realized using MOCVD showed $\sim$2.5 times larger quantum efficiency rollover threshold as compared to the conventional stepped-MQW-LED [29]. This improvement has been attributed to the reduced polarization field, and reduced band bending in the graded-MQW based active region.

In this study, we design graded-MQW active region to achieve uniform carrier distribution with high radiative recombination in the active region, without resorting to AlGaN-based EBL or QW-barrier large bandgap insertion layers. In agreement with the obtained simulation results, extended quantum efficiency rollover threshold was obtained for graded-MQW-LED as compared to the conventional stepped-MQW-LED. To investigate the effect of grading profile on carrier distribution and recombination rate considering growth implementation, we have studied various graded schemes, i.e., the linear, parabolic and Fermi-function profiles in the simulation. A graded-MQW-LED was grown on c-plane sapphire template substrate using plasma assisted molecular beam epitaxy (PAMBE), and the efficiency droop was compared with a stepped-MQW-LED. Micro-LEDs with circular mesa diameter (D) of 80 $\mu$m were fabricated.

## 2. Design and Simulation Results

Fig. 1 shows the designed layer structures for the stepped- and graded-MQW LEDs on sapphire-based GaN template substrate. The LED structures consist of 650 nm thick n-GaN layer,

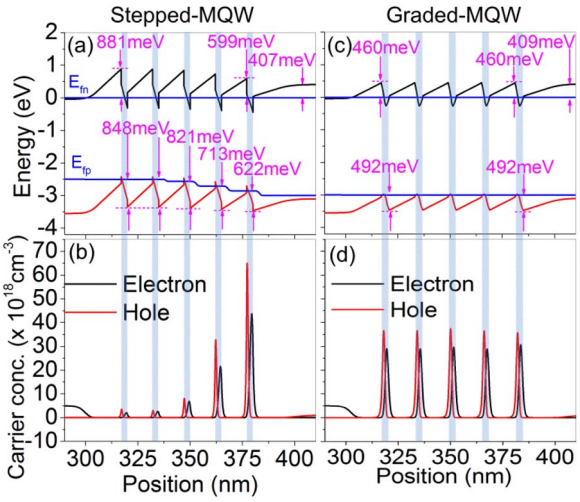


Fig. 2. Respective energy band diagram and carrier concentration at 3 V bias voltage for stepped-MQW in (a) and (b) and for graded MQW-LED (c) and (d), respectively (shaded regions represent the QW; QW1–5 are positioned from left to right).

followed by five pairs of QWs and a 100 nm p-GaN cap layer. The active regions of the simulated stepped-MQW-LED consist of five pairs of $In_{0.2}Ga_{0.8}N$ (3 nm)/GaN (12 nm), while that of graded-MQW consists of GaN (12 nm)/$In_{0\rightarrow0.2}Ga_{1\rightarrow0.8}N$ (1.75 nm)/$In_{0.2}Ga_{0.8}N$ (0.5 nm)/$In_{0.2\rightarrow0}Ga_{0.8\rightarrow1}N$ (1.75 nm)/GaN (12 nm) QWs, respectively. Simulations were performed considering energy band alignment, comparison of carrier densities in MQW, spatial wavefunction overlap, electric field, and recombination rates using the NEXTNANO software [36]. The active region of simulated LED structure was assigned an unintentional background electron carrier concentration of $1 \times 10^{16}$ $cm^{-3}$ to prevent doping induced non-radiative recombination, and impurity scattering. The conduction-to-valance-band offsets ratio, $\Delta E_c/\Delta E_v$, was taken as 70 : 30 for the material system [37]. Band parameters for ternary alloy InGaN were calculated based on *Vegard's* law [38]. The electron and hole, effective masses, and the elastic, piezoelectric and deformation potentials for the ternary compound were extrapolated linearly [39]. The Arora model was used to obtain doping dependent mobilities for the intrinsic InGaN [40]

$$u(T, N_i) = u_{\min}^{n,p}\left(\frac{T}{T_o}\right)^{\alpha_m^{n,p}} + \frac{u_d^{n,p}\left(\frac{T}{T_o}\right)^{\alpha_d^{n,p}}}{1 + \left(\frac{N_D+N_A}{N_0^{n,p}\left(\frac{T}{T_o}\right)^{\alpha_N^{n,p}}}\right)^{A_a^{n,p}\left(\frac{T}{T_o}\right)^{\alpha_a^{n,p}}}}$$

where $u_{\min}$, $u_d$, $\alpha_m$, $\alpha_d$, $\alpha_N$, $\alpha_a$, and $N_0$ are Arora model fitting parameters [41]. $N_A + N_D$ is the total concentration of ionized impurities.

Fig. 2(a) shows the calculated energy band diagram with the electrons and holes quasi-Fermi-levels ($E_{fn}$ and $E_{fp}$) for the stepped-MQW-LED at a forward bias of 3 V and at room temperature. Abruptness at the polarization mismatch hetero-interfaces (GaN/InGaN stepped MQW) leads to large sheet charges at the interfaces, which result in triangular shaped QW as shown in Fig. 2(a). For simplicity, five stacks of QW along the [0001] growth direction are indicated by QW1–5 with QW1 adjacent to the n-GaN and QW5 adjacent to p-GaN. The $E_{fp}$ in the stepped-MQW-LED mimics a staircase pattern with effective potential barriers of 848 meV, 848 meV, 821 meV, 713 meV, and 622 meV in QW1–5 respectively. This leads to the non-uniform distribution of hole concentrations with maximum and minimum values in QW5 and QW1, correspondingly [see Fig. 2(b)]. Non-uniform electron concentration among the five QWs was also obtained due to overall downward bending of conduction band (CB) along the growth direction.

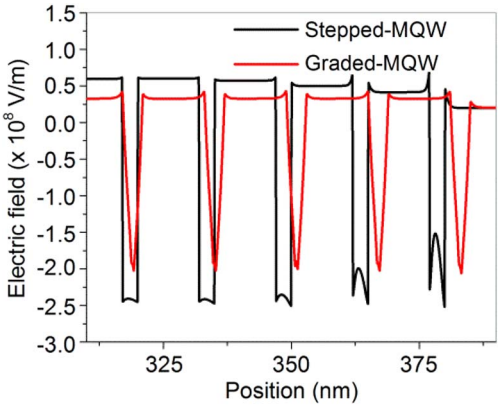


Fig. 3. Calculated electric field of stepped-MQW-LED and graded-MQW-LED under the bias of 3 V.

Thus, most electrons get accumulated in the QW5. Such non-uniform distribution of carrier concentrations among the QWs in the active region will be detrimental for device performance.

A graded-MQW scheme was conceived and optimized in this work. Fig. 2(c) shows the energy band diagram of a graded-MQW-LED in which the 3 nm thick stepped QW was replaced by 1.75 nm linearly down-graded indium composition layer, 0.5-nm-thick $In_{0.2}Ga_{0.8}N$ and 1.75 nm linearly up-graded indium composition layer, which resulted in a reduced polarization mismatch. This leads to the absence of staircase $E_{fp}$ profile. Moreover, since the active region and p-GaN see equal potential barrier of 492 meV, the uniform distribution of carriers are greatly facilitated into the five quantum wells in the linearly graded-MQW-LED as shown in Fig. 2(d). In addition, improved spatial overlap for graded-MQW (for QW3 19.6%) as compared to stepped-MQW (for QW3 4.9%) was obtained. To shed light on the role of a thin compositionally graded layer in reducing the abruptness of polarization mismatch in achieving uniform carrier distribution in the active region, the electrical field profile was examined. As is evident in Fig. 3, we obtained lower electric fields in the active region of the graded-MQW-LED as compared to that of stepped-MQW-LED, resulting in a lower band bending and hence a more uniform carrier distributions within the active region of graded-MQW-LED.

In general, compositional grading in InGaN graded-layers is experimentally implemented by employing change in growth temperature [26], [28]–[31]. However, the resulting grading in composition may not be perfectly linear [42]–[44]. Also, the role of non-linear grading profiles on carrier distribution in MQW based LEDs remain unaddressed [45], [46]. Thus, we further investigated the effect of different grading profile, such as linear, parabolic, and Fermi-function numerically, on the carrier distribution and radiative recombination for the graded-MQW-LED design compared to the stepped-MQW-LED.

As shown in Fig. 4(a), all three grading schemes resulted in comparable radiative recombination across all five QWs while stepped-MQW-LED showed disparate radiative recombination as large as three orders of comparing between QW1 and QW5. Moreover, graded-MQW-LED with parabolic compositional profile attained the highest radiative recombination rate of $3.3 \times 10^{29}$ $cm^{-3}s^{-1}$ which is attributed to its higher electron and hole concentrations obtained in QW1–5 as compared to linear and Fermi-function profiles [see Fig. 4(b) and (c)]. The simulated results showed that the fundamental transition in all the QWs (QW1–5), with parabolic profile, was at 2.89 eV with 3 V forward bias. In order to verify the highest radiative rate with parabolic profile, we further examined electric field in the active regions with different grading profiles. As shown in Fig. 4(d), the lowest electrical field was obtained using parabolic profile based graded-MQW, and as a consequence, lower band bending and higher electron-hole wavefunction overlap was obtained. Thus, the parabolic shape has a high radiative rate as a result of high carrier concentration and high electron-hole wavefunction overlap.

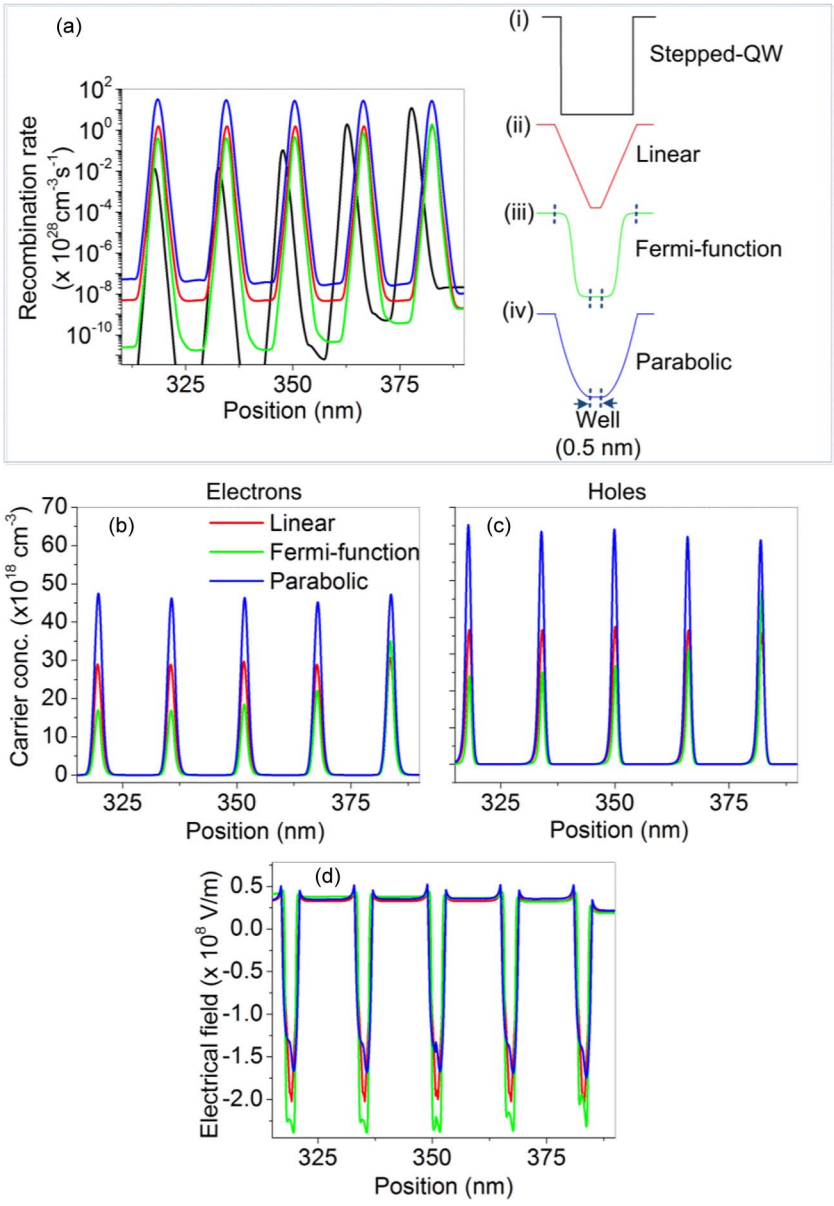


Fig. 4. (a) Radiative recombination rate of compositionally graded-MQW-LEDs with different indium grading schemes (linear, Fermi-function, parabolic) and stepped-MQW-LED (schematics of bandgap profile for different schemes were also shown). Electrons (b) and hole (c) concentrations in graded-MQW-LEDs with different compositional grading profile (linear, Fermi-function, and parabolic). (d) The calculated electric field of graded-MQW-LED with the linear (red curve), Fermi-function (green curve), and parabolic (blue curve) grading profiles under the bias of 3 V.

## 3. Device Implementation and Measurements

For experimental verification of the advantageous effect of the insertion of compositionally graded layers in graded-MQW-LED, it is important to consider suitable growth technology for implementing graded-MQW-LED. Comparing with MOCVD, PAMBE growth process is advantageous for the growth of thin (few monolayers) compositionally graded InGaN layer since it is capable of low growth rate process, and equipped with *in situ* reflection high-energy electron diffraction (RHEED) for monitoring surface growth condition at monolayer scale.

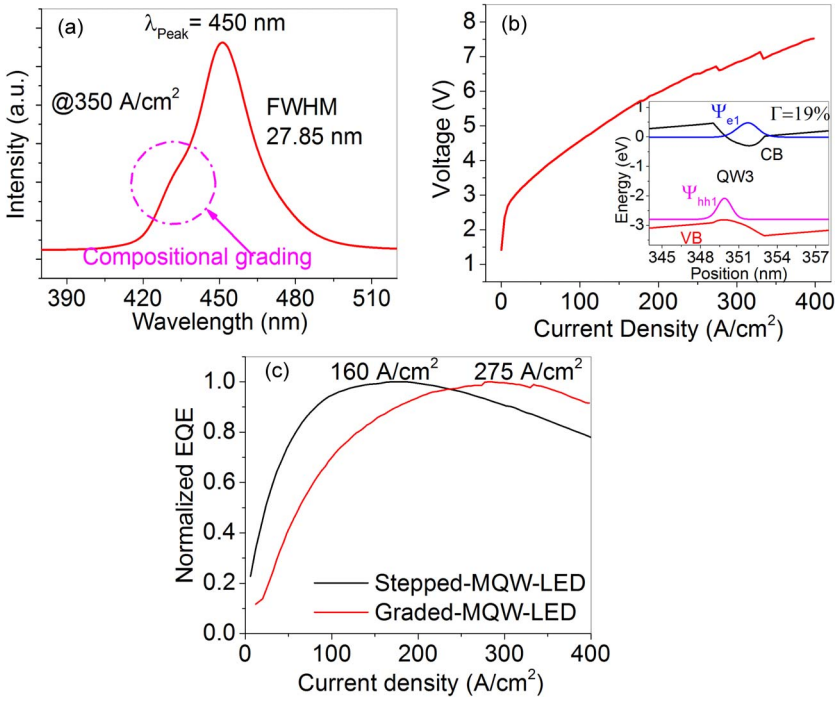


Fig. 5. (a) EL spectra of graded-MQW-LED at 350 A/cm$^2$. (b) Typical J–V characteristics of graded-MQW-LED (inset shows energy band diagram of graded-QW3 with parabolic profile at bias voltage of 3 V). (c) Normalized EQE of graded MQW-LED and stepped-MQW-LED.

Thus, we have implemented a graded-MQW-LED by using PAMBE, consisting of a 650 nm thick n-GaN layer, followed by five pairs of graded-QWs, and a 100 nm p-GaN cap layer. In the graded-QW region, the undoped 12 nm GaN quantum barriers were grown under stoichiometric conditions using Ga beam equivalent pressure (BEP) of $6.0 \times 10^{-8}$ Torr at 595 °C. The indium flux $8.5 \times 10^{-8}$ Torr and nitrogen plasma conditions, i.e., flow rate 0.4 sccm and RF power 200 W were kept constant during the well and graded-layer growth. An interruption time of 1 min was provided for ramping the growth temperature from 595 to 585 °C, and *vice-versa*, before the growth of 1.75 nm graded-InGaN cladded 0.5 nm InGaN QW. The interruption time was optimized in separate growth experiments utilizing RHEED technique by measuring the specular spot intensity for ensuring complete desorption of excess gallium before the growth of graded—and well-layers. The growth kinetics for graded-MQW were also optimized to fulfil $(f_{Ga} + f_{In}) > f_N$, $(f_{Ga} < f_N)$ conditions, under which indium composition $x$ in the InGaN alloy is governed by following expression [47], [48]

$$x = \frac{f_N - f_{Ga}}{f_N}$$

where, $f_{Ga,In,N}$ are the incident fluxes of Ga, In, and N. According to the above equation, the required indium composition can be varied by changing the $f_{Ga}$ at a given growth temperature. Therefore, to realize graded indium profile at the bottom, and top graded-layers, we changed the gallium BEP between $6.0 \times 10^{-8}$ Torr and $4.5 \times 10^{-8}$ Torr by varying the effusion cell temperature linearly. It is expected that a parabolic compositional grading is achieved with linear variation in gallium effusion cell temperature.

Comparing growth aspects, our EBL-less design based on graded-MQW-LED is simpler to implement as compared to the previously proposed EBL-less design based on AlGaN-in-active-region [20]–[22]. In order to avoid dissociation of InGaN quantum well, AlGaN layers need to be grown at lower growth temperature (around growth temperature of InGaN). At this temperature,

grown AlGaN leads to poor crystal quality, in particular, high defect density. However, our EBL-less design overcomes such ambiguity in the growth process. Fig. 5(a) shows electroluminescence spectra of graded-MQW-LED having peak emission wavelength of 450 nm with full-width-half-maximum (FWHM) of 27.85 nm at injection current density 350 A/cm$^2$. Also, side hump is observed at around 430 nm marked with a dotted circle, which point towards the availability of lower Indium compositional region within the well i.e. incorporated graded-layer. Fig. 5(b) shows the injection current density vs. the DC bias characteristics for graded-MQW-LED with current density of about $\sim$400 A/cm$^2$ at 7.5 V. Fig. 5(b) inset shows the band diagram of the graded-QW with parabolic profile along with its corresponding electron and hole wavefunction having spatial overlap $(\Gamma_{e\_hh})$ of 19%.

Further, external quantum efficiencies (EQEs) for graded-MQW-LED and stepped-MQW-LED were also evaluated by measuring the light output powers under different injection current densities. The advantage of the graded-MQW-LED is evident in the normalized external quantum efficiency plot in Fig. 5(c). The stepped-MQW-LED attained maximum efficiency at injection level of 160 A/cm$^2$. On the other hand, the maximum efficiency of graded-MQW-LED was attained at injection level of 275 A/cm$^2$. Hence, the onset of efficiency rollover for graded-MQW-LED occurred at higher injection current level as compared to the stepped-MQW-LED. The extended droop roll-over for graded-MQW-LED can be attributed to the reduced band bending, uniform carrier distribution in the active region and non-overcrowding of carriers in the last-QW closest to the p-GaN layer.

As the carriers are evenly distributed across all QWs, the last graded-QW has a lower carrier concentration compared to that of the stepped-QW, resulting in the alleviation of the undesired carrier leakage and *Auger* recombination, and thus contributed to the extended efficiency roll-over effect. The evenly distributed carriers in all QWs achieved mainly due to the reduced polarization field by implementing compositionally graded-layer, and improved hole injection into the active region by using EBL-less design.

## 4. Conclusion

In conclusion, we have compared LED designs based on graded-MQW and conventional stepped-MQW; the graded-MQW having enhanced carrier uniformity due to reduced polarization field as obtained numerically. Different grading schemes based on linear, parabolic and Fermi-function were taken into account. In particular, graded-MQW-LED with parabolic grading profile showed the highest radiative recombination rate with uniform carrier distribution. Our work highlights the realization of optimized graded-MQW-LED by surface stoichiometry monitoring using RHEED based on the controllable growth rate in PAMBE. The efficiency droop in the implemented graded-MQW-LED occurred at higher injection levels $(\sim$275 A/cm$^2)$ as compared to a stepped-MQW-LEDs $(\sim$160 A/cm$^2)$, thus demonstrating the effectiveness of our EBL-less graded active region design.

## References

[1] Y. C. Shen *et al.*, "Auger recombination in InGaN measured by photoluminescence," *Appl. Phys. Lett.*, vol. 91, no. 14, Oct. 2007, Art. ID. 141101.
[2] B. Monemar and B. E. Sernelius, "Defect related issues in the "current roll-off" in InGaN based light emitting diodes," *Appl. Phys. Lett.*, vol. 91, no. 18, Oct. 2007, Art. ID. 181103.
[3] H. P. Zhao, G. Y. Liu, R. A. Arif, and N. Tansu, "Current injection efficiency induced efficiency-droop in InGaN quantum well light-emitting diodes," *Solid State Electron.*, vol. 54, no. 10, pp. 1119–1124, Oct. 2010.
[4] S. H. Park, "Crystal orientation effects on electronic properties of Wurtzite InGaN/GaN quantum wells," *J. Appl. Phys.*, vol. 91, no. 12, pp. 9904–9908, Jun. 2002.
[5] S. H. Park and S. L. Chuang, "Crystal-orientation effects on the piezoelectric field and electronic properties of strained Wurtzite semiconductors," *Phys. Rev. B, Condens. Matter*, vol. 59, no. 7, pp. 4725–4737, Feb. 1999.
[6] I. H. Brown *et al.*, "Time evolution of the screening of piezoelectric fields in InGaN quantum wells," *IEEE J. Quantum Electron.*, vol. 42, no. 12, pp. 1202–1208, Nov./Dec. 2006.

[7] M. H. Kim *et al.*, "Origin of efficiency droop in GaN-based light-emitting diodes," *Appl. Phys. Lett.*, vol. 91, no. 18, Oct. 2007, Art. ID. 183507.
[8] B. C. Lin *et al.*, "Advantages of blue LEDs with graded-composition AlGaN/GaN superlattice EBL," *IEEE Photon. Technol. Lett.*, vol. 25, no. 21, pp. 2062–2065, Nov. 2013.
[9] G. Y. Liu, J. Zhang, C. K. Tan, and N. Tansu, "Efficiency-droop suppression by using large-bandgap AlGaInN thin barrier layers in InGaN quantum-well light-emitting diodes," *IEEE Photon. J.*, vol. 5, no. 2, Apr. 2013, Art. ID. 2201011.
[10] B. C. Lin *et al.*, "Hole injection and electron overflow improvement in InGaN/GaN light-emitting diodes by a tapered AlGaN electron blocking layer," *Opt. Exp.*, vol. 22, no 1, pp. 463–469, Jan. 2014.
[11] J. P. Liu *et al.*, "Barrier effect on hole transport and carrier distribution in InGaN/GaN multiple quantum well visible light-emitting diodes," *Appl. Phys. Lett.*, vol. 93, no. 2, Jul. 2008, Art. ID. 021102.
[12] R. M. Lin *et al.*, "Inserting a p-InGaN layer before the p-AlGaN electron blocking layer suppresses efficiency droop in InGaN-based light-emitting diodes," *Appl. Phys. Lett.*, vol. 101, no. 8, Aug. 2012, Art. ID. 081120.
[13] Z. Q. Li, M. Lestrade, Y. G. Xiao, and Z. S. Li, "Improvement of performance in p-side down InGaN/GaN light-emitting diodes with graded electron blocking layer," *Jpn. J. Appl. Phys.*, vol. 50, no. 8R, Aug. 2011, Art. ID. 080212.
[14] H. J. Kim *et al.*, "Improvement of quantum efficiency by employing active-layer-friendly lattice-matched InAlN electron blocking layer in green light-emitting diodes," *Appl. Phys. Lett.*, vol. 96, no. 10, Mar. 2010, Art. ID. 101102.
[15] S. Choi *et al.*, "Improvement of peak quantum efficiency and efficiency droop in III-nitride visible light-emitting diodes with an InAlN electron-blocking layer," *Appl. Phys. Lett.*, vol. 96, no. 22, May 2010, Art. ID. 221105.
[16] S. C. Wang *et al.*, "Enhanced performance of GaN-based light-emitting diodes by using a p-InAlGaN/GaN superlattice as electron blocking layer," *J. Mod. Opt.*, vol. 60, no. 21, pp. 2013–2018, Dec. 2013.
[17] X. P. Yu, G. H. Fan, S. W. Zheng, B. B. Ding, and T. Zhang, "Performance of blue LEDs with n-AlGaN/n-GaN superlattice as electron-blocking layer," *IEEE Photon. Technol. Lett.*, vol. 26, no. 11, pp. 1132–1135, Jun. 2014.
[18] J. H. Park *et al.*, "Enhanced overall efficiency of GaInN-based light-emitting diodes with reduced efficiency droop by Al-composition-graded AlGaN/GaN superlattice electron blocking layer," *Appl. Phys. Lett.*, vol. 103, no. 6, Aug. 2013, Art. ID. 061104.
[19] H. Y. Ryu *et al.*, "Efficiency and electron leakage characteristics in GaN-based light-emitting diodes without AlGaN electron-blocking-layer structures," *IEEE Photon. Technol. Lett.*, vol. 23, no. 24, pp. 1866–1868, Dec. 2011.
[20] L. W. Cheng and S. D. Wu, "Performance enhancement of blue InGaN light-emitting diodes with a GaN–AlGaN–GaN last barrier and without an AlGaN electron blocking layer," *IEEE J. Quantum Electron.*, vol. 50, no. 4, pp. 261–266, Apr. 2014.
[21] J. Y. Xiong, Y. Q. Xu, S. W. Zheng, G. H. Fan, and T. Zhang, "Advantages of blue InGaN light-emitting diodes without an electron-blocking layer by using AlGaN step-like barriers," *Appl. Phys. A—Mater. Sci. Process.*, vol. 114, no. 2, pp. 309–313, Feb. 2014.
[22] J. Y. Chang *et al.*, "Reduced efficiency droop in blue InGaN light-emitting diodes by thin AlGaN barriers," *Opt. Lett.*, vol. 39, no. 3, pp. 497–500, Feb. 2014.
[23] Y. Y. Zhang, G. H. Fan, Y. A. Yin, and G. R. Yao, "Performance enhancement of blue light-emitting diodes without an electron-blocking layer by using special designed p-type doped InGaN barriers," *Opt. Exp.*, vol. 20, no. S1, pp. A133–A140, Jan. 2012.
[24] H. Y. Ryu and J. M. Lee, "Effects of two-step Mg doping in p-GaN on efficiency characteristics of InGaN blue light-emitting diodes without AlGaN electron-blocking layers," *Appl. Phys. Lett.*, vol. 102, no. 18, May 2013, Art. ID. 181115.
[25] S. H. Park, D. Ahn, and J. W. Kim, "High-efficiency staggered 530 nm InGaN/InGaN/GaN quantum-well light-emitting diodes," *Appl. Phys. Lett.*, vol. 94, no. 4, Jan. 2009, Art. ID. 041109.
[26] H. P. Zhao *et al.*, "Growths of staggered InGaN quantum wells light-emitting diodes emitting at 520–525 nm employing graded growth-temperature profile," *Appl. Phys. Lett.*, vol. 95, no. 6, Aug. 2009, Art. ID. 061104.
[27] N. Tansu *et al.*, "III-Nitride Photonics," *IEEE Photon. J.*, vol. 2, no. 2, pp. 241–248, Apr. 2010.
[28] C.-Y. Chang, H. Li, and T.-C. Lu, "High efficiency InGaN/GaN light emitting diodes with asymmetric triangular multiple quantum wells," *Appl. Phys. Lett.*, vol. 104, no. 9, Mar. 2014, Art. ID. 09111.
[29] L. H. Zhu *et al.*, "Efficiency droop improvement in InGaN/GaN light-emitting diodes by graded-composition multiple quantum wells," *IEEE Photon. J.*, vol. 5, no. 2, Apr. 2013, Art. ID. 8200208.
[30] W. Liu *et al.*, "Influence of GaN barrier thickness on optical properties of in-graded InGaN/GaN multiple quantum wells," *Appl. Phys. Exp.*, vol. 6, no. 8, Aug. 2013, Art. ID. 081001.
[31] H. P. Zhao *et al.*, "Approaches for high internal quantum efficiency green InGaN light-emitting diodes with large overlap quantum wells," *Opt. Exp.*, vol. 19, no. S4, pp. A991–A1007, Jul. 2011.
[32] Y. J. Zhao *et al.*, "High-power blue-violet semipolar (2021) InGaN/GaN light-emitting diodes with low efficiency droop at 200 A/cm$^2$," *Appl. Phys. Exp.*, vol. 4, no. 8, Aug. 2011, Art. ID. 082104.
[33] Y. J. Zhao *et al.*, "Green semipolar (2021) InGaN light-emitting diodes with small wavelength shift and narrow spectral linewidth," *Appl. Phys. Exp.*, vol. 6, no. 8, Jun. 2013, Art. ID. 062102.
[34] R. M. Farrell, E. C. Young, F. Wu, S. P. DenBaars, and J. S. Speck, "Materials and growth issues for high-performance nonpolar and semipolar light-emitting devices," *Semicond. Sci. Technol.*, vol. 27, no. 2, Feb. 2012, Art. ID. 024001.
[35] Y. J. Zhao *et al.*, "Indium incorporation and emission properties of nonpolar and semipolar InGaN quantum wells," *Appl. Phys. Lett.*, vol. 100, no. 20, May 2012, Art. ID. 201108.
[36] S. Birner *et al.*, "Nextnano: General purpose 3-D simulations," *IEEE Trans. Electron Devices*, vol. 54, no. 9, pp. 2137–2142, Sep. 2007.
[37] J. Piprek and S. Nakamura, "Physics of high-power InGaN/GaN lasers," *Proc. Inst. Elect. Eng.—Optoelectron.*, vol. 149, no. 4, pp. 145–151, Aug. 2002.
[38] J. Piprek, *Nitride Semiconductor Devices: Principles and Simulation*. Hoboken, NJ, USA: Wiley, 2007.
[39] I. Vurgaftman and J. R. Meyer, "Electron band structure parameters," in *Nitride Semiconductor Devices: Principles and Simulation*. Hoboken, NJ, USA: Wiley, 2007, p. 13.

[40] N. D. Arora, J. R. Hauser, and D. J. Roulston, "Electron and hole mobilities in silicon as a function of concentration and temperature," *IEEE Trans. Electron Devices*, vol. ED-29, no. 2, pp. 292–295, Feb. 1982.
[41] E. Bellotti and F. Bertazzi, *Transport Parameters for Electrons and Holes*. Weinheim, Germany: Wiley-VCH Verlag GmbH & Co. KGaA, 2007.
[42] Y. R. Wu, R. Shivaraman, K. C. Wang, and J. S. Speck, "Analyzing the physical properties of InGaN multiple quantum well light emitting diodes from nano scale structure," *Appl. Phys. Lett.*, vol. 101, no. 8, Aug. 2012, Art. ID. 083505.
[43] C. Kisielowski, Z. Liliental-Weber, and S. Nakamura, "Atomic scale indium distribution in a GaN/In0.43Ga0.57N/Al0.1Ga0.9N quantum well structure," *Jpn. J. Appl. Phys. 1, Regul. Rap. Short Notes*, vol. 36, no. 11, pp. 6932–6936, Nov. 1997.
[44] T. P. Bartel and C. Kisielowski, "A quantitative procedure to probe for compositional inhomogeneities in InxGa1-xN alloys," *Ultramicroscopy*, vol. 108, no. 11, pp. 1420–1426, Oct. 2008.
[45] S. H. Park *et al.*, "Comparison of light emission in InGaN/GaN light-emitting diodes with graded, triangular, and parabolic quantum-well structures," *J. Korean Phys. Soc.*, vol. 60, no. 3, pp. 505–508, Feb. 2012.
[46] P. M. McBride, Q. M. Yan, and C. G. Van de Walle, "Effects of in profile on simulations of InGaN/GaN multi-quantum-well light-emitting diodes," *Appl. Phys. Lett.*, vol. 105, no. 8, Aug. 2014, Art. ID. 083507.
[47] H. J. Chen, R. M. Feenstra, J. Northrup, J. Neugebauer, and D. W. Greve, "Indium incorporation and surface segregation during InGaN growth by molecular beam epitaxy: Experiment and theory," *MRS Internet J. Nitride Semicond. Res.*, vol. 6, no. 11, pp. U1–U12, 2001.
[48] R. Averbeck and H. Riechert, "Quantitative model for the MBE-growth of ternary nitrides," *Phys. Stat. Sol. (A)—Appl. Res.*, vol. 176, pp. 301–305, Nov. 1999.